

Rectifier Load Analysis for Electric Vehicle Wireless Charging System

Dhanesh S. Bhamare¹, R. V. S. Ramkrishana²

¹Student at Electrical Engineering Department, Gokhale Education Society's R. H. Sapat College of Engineering, Nashik – 422005;

²Professor at Electrical Engineering Department, Gokhale Education Society's R. H. Sapat College of Engineering, Nashik – 422005;

Abstract - This paper presents the analysis of rectifier load used for electrical vehicle wireless charging system, along with its application on network with load estimation method. The rectifier load model is developed using its equivalent circuit. A compensation network style technique is planned & used for the rectifier load analysis, also, a secondary load estimation technique and a primary load estimation technique area unit shows solely measured voltages and contemplate the influence of the rectifier load. The associate work unit wireless charging model is developed, and results & simulations are performed using equivalent load area unit usually properly calculated on conditions of various system load resistances, rectifier input inductances, DC voltages, and mutual-inductances. The results & simulations show that rectifier load equivalent inductance can affect system performances, and thus the developed methods have good accuracy.

Keywords: Wireless charging system, compensation network style, rectifier load, load estimation.

1. INTRODUCTION

Electric Vehicle (EV) Wireless Charging System (WCS) has the benefits of convenience, space-saving, etc. So, it's attracted tons of attention. In recent years, rule, operation characteristics, system style, and management technique of every stationary and dynamic wireless heat unit charging systems are studied and applied to some demonstrations[1]. In applications for unit wireless charging, rectifier and output filter condenser are required to convert the high frequency AC to DC, therefore on charge the facility battery. Rectifier then the circuit once it is sometimes kind of a pure resistance load to vogue the system or management strategy[2]. A customary manner is exploitation the constant $8/\pi^2$ to form identical relationship between the rectifier input resistivity then the system load resistance[4][5]. However, stray parameters and non-ideal behaviors of the devices can become obvious at the high frequency vary[5]. Also, rectifier input resistivity is typically stricken with the input inductance and alternative parameters. So, it'll bring some deviations, if solely considering WCS rectifier input resistivity as a pure resistance. Actually, rectifier input resistivity of labor unit wireless charging system contains each resistance half and inductance half [6]. It is typically expressed as a series of identical resistance and also an equivalent inductance[5][6]. Though there has not been a cheap technique to urge the equivalent load resistivity of WCS rectifier, some existing researches are often useful. supported the on and off states[6], the rectifier and its connected inductance and capacitance circuits are typically delineate by the state area model[7], considering the stray resistances and diode forward drop. Then, the expressions of the connected voltages and currents are obtained at intervals the time domain, frequency domain, or complicated frequency

domain[8], which may be used for the analysis of WCS rectifier equivalent load resistivity. Besides, non-linear change functions gate simulations might even be adopted to review the issue[9]. The non-linear method of rectifier load can bring some difficulties to system compensation network style. In most cases, a pure resistance is employed to precise the rectifier load[11-13]. However, the operation modes of WCS rectifier load can have an impact on the operating states of compensation network[14]. So, actual equivalent input resistivity of WCS rectifier load need to be thought of, whereas planning the compensation networks. Load estimation of WCS has two-faced identical downside. Effects of the rectifier load might complicate the equations used for load estimation[15], and cause the increasing of calculation and management complexness. Hence, a pure resistance load is simply about used for several of the load estimation, detection, or best load pursuit[16]. Another scenario is that the voltages and currents are sometimes each measured for load estimation, therefore on calculate the impedances at intervals the primary aspect[16]. Since the voltage and current sensors or probes have totally different section delays at the high frequency vary, some deviations might even be introduced into the estimation methods. Also, the hardness of the estimation technique is awfully necessary. It is typically analyzed through parameter derivation, root locus, Nyquist curve, Bode graph, or directly hard the results on conditions of parameter variations[17]. Supported the previous researches, a cheap technique to quantitatively analyze the load of WCS rectifier is suggests at intervals the paper first. the facility for load are typically severally calculated through the parameters of the rectifier circuit, the implications of the rectifier non-linear method are taken into count to estimate the system load resistance. The planned load estimation technique measures the voltage & current & Calculates power.

2. RECTIFIER LOAD ANALYSIS AND CALCULATION

Full-bridge diode rectifier is that the foremost normally used topology in work unit wireless eleven systems. Also, dual-side LCC compensation networks which will offer many applicable style degrees of freedom to understand many system performance indicators at an identical time. Moreover, it is usually designed to make the system resonant frequency freelance of the load condition[10]. Therefore, we've a scope to design the rectifier load on the concept of this type of topology.

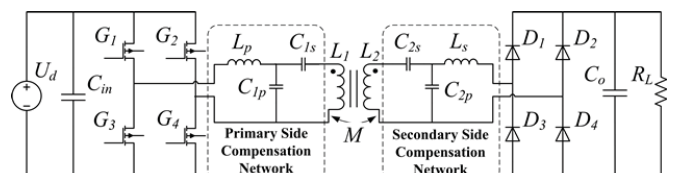


Fig. 1. Electric Vehicle wireless charging system with full-bridge diode rectifier and dual-side LCC compensation networks.

Fig.1 shows the work unit wireless charging system with full-bridge diode rectifier and dual-side LCC compensation networks; wherever, U_d is DC voltage source; the high frequency converter consists of G_1 - G_4 , and thus the full-bridge rectifier consists of D_1 - D_4 ; the first aspect compensation network consists of disk, C_{1s} , and C_{1p} ; the secondary aspect compensation network consists of L_s , C_{2s} , and C_{2p} ; L_1 and L_2 are self-inductances of the transmitting coil and receiving coil; M is mutual-inductance between them; C_{in} and C_o are system input and output filter condensers; R_L is system load resistance. It need to be detected that the WCS load is a work unit power battery at intervals the sensible case, that behaves as a voltage supply series with its parasitic resistance. However, the power battery is often kind of a load resistance R_L ; the worth of this equivalent resistance is usually calculated by the voltage on the power battery divided by this flowing through it. Moreover, the full-bridge rectifier, its input inductance, output filter capacitor, and thus the load resistance are along outlined as a results of the rectifier circuit. Though subsequent analysis is conducted and supported the precise system, they are usually extended to applications on different rectifier and compensation network topologies.

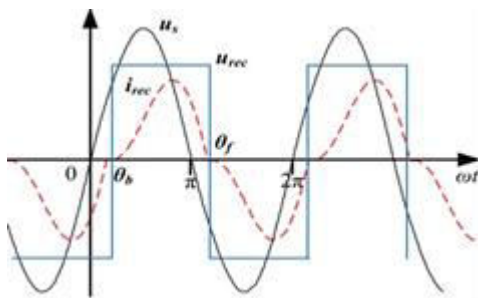


Fig. 2. Schematic waveforms of the supply voltage, rectifier input voltage and current.

Thus on calculate rectifier equivalent input resistance, we tend to foremost need to be compelled to research the voltages and currents of rectifier circuit, that is shown in Fig.2; where, North American country is that the voltage on C_{2p} , which may be a wave, and will be treated as a results of the voltage supply of the rectifier circuit; u_{rec} and i_{rec} are rectifier input voltage and current; the beginning time folks positive half-cycle is chosen as a results of the coordinate zero of axis. θ_b and θ_f are begin and finish section angles of u_{rec} and i_{rec} . So, $\theta_f = \theta_b + \pi$. Also, the rectifier input inductance L_s need to be massive enough to stay the rectifier operating inside the continual conductivity mode (CCM), thus on avoid large current peaks inside the diodes. Hence, solely CCM states are shown in Fig.2, and mentioned throughout this paper. Besides, the steady state waveforms of u_{rec} and i_{rec} are given in Fig.2, once solely one or two of fluctuations exist on the voltage of the output capacitor C_o and thus the drop on R_{Co} is not considerable. So, u_{rec} are typically more or less delineated as a square wave. Fig.2 suggests that the analyzed waveform of rectifier input current i_{rec} has some distortion, due to the result of the rectifier input inductance. This makes the elemental wave of i_{rec} lags behind the one altogether i_{rec} . So, the rectifier input resistance doesn't simply embody resistance element, however conjointly contains a specific

inductance element. Moreover, Fig.2 shows that the positive and negative half-cycles are radial for all the voltage and current waveforms. Hence, we tend to easily need to be compelled to believe the positive half-cycle, and thus the negative half-cycle are typically obtained from the symmetry. Fig.3 shows the equivalent circuit of the rectifier circuit inside the positive $[*f_{r1}]$ cycle, considering the stray parameters and thus the diode forward voltage drop; wherever, u_{dio} represents the diode forward voltage drop; R_{dio} is diode conductivity resistance; R_L and R_{Co} are stray resistances of L_s and C_o , respectively; u_d and i_d are load voltage and current.

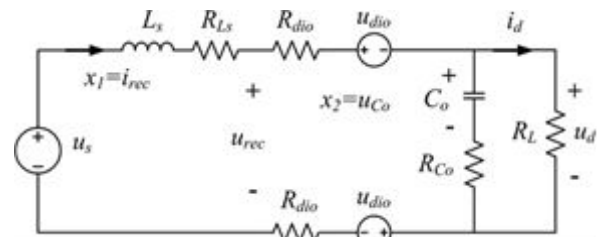


Fig. 3. Equivalent circuit of the rectifier circuit within the positive 0.5 cycle.

Supported the equivalent circuit, i_{rec} is printed as state variable x_1 , then the voltage on C_o is printed as state variable x_2 . u_s & u_d is treated as a result of the output variable. So, state house equation of the rectifier circuit inside the positive 0.5 cycle is given by (1a).

$$\begin{bmatrix} \dot{x}'_1 \\ \dot{x}'_2 \end{bmatrix} = A \begin{bmatrix} x_1 \\ x_2 \end{bmatrix} + B \begin{bmatrix} u_s \\ u_{dio} \end{bmatrix}, y = C \begin{bmatrix} x_1 \\ x_2 \end{bmatrix} \quad (1a)$$

Where, impedance matrixes A, B, and C are given by equation (1b).

Fehler!Fehler!Fehler!Fehler!

$$B = \begin{bmatrix} \text{Fehler!} & \text{Fehler!} \\ 0 & 0 \end{bmatrix}, C = [\text{Fehler!} \quad 1 - \text{Fehler!}] \quad (1b)$$

Then, the input variables and thus the initial values of the state variables area unit given by (2), in line with the schematic waveforms in Fig.2; where, ω is system angle frequency; the diode forward drop is treated as a unbroken worth V_{dio} . Since solely a number of fluctuations exist on the voltage of C_o and thus the drop on R_{Co} is negligible, their influences area unit usually unnoticed, and thus the initial worth of x_2 area unit usually on the brink of kind of a DC voltage variable V_d . Also, value of u_s is printed as V_s , and it'll be suffering from WCS parameters, like supply voltage, mutual-inductance, etc. however the amplitudes of u_{rec} and i_{rec} area unit proportional to V_s . So, V_s area unit usually treated as an identified variable.

$$u_{s+} = V_s \sin(\omega t + \theta_b), u_{dio} = V_{dio}, x_+(0) = [0, V_d]^T \quad (2)$$

Furthermore, V_d and θ_b need to be calculated to derive the values for state space equation variable. On the wireless charging system operating parameters, the magnitude of V_{dio} and thus the voltage drops on R_{dio} and R_{Ls} area unit lesser than those of V_d and V_d . So, the voltage on L_s is around like $V_s \sin \theta - V_d$, and thus the expression of i_{rec} area unit

typically given by (3), the voltage across inductor & current through inductor,

$$i_{rec} = \frac{1}{\omega L_s} \int_{\theta_b}^{\theta} (V_s \sin \theta - V_d) d\theta \quad (3)$$

As shown in Fig.2, $i_{rec}=0$, once $\theta = \theta_f = \theta_b + \pi$. So, one equation between V_d and θ_b typically got and given by (4).

$$V_d = (2V_s \cos \theta_b) / \pi \quad (4)$$

The DC load current I_d can be given as in equation 5,

$$I_d = \frac{1}{\pi \omega L_s} \int_{\theta_b}^{\theta_b + \pi} \int_{\theta_b}^{\theta} (V_s \sin \theta - V_d) d\theta = [(V_s(2\sin \theta_b + \pi \cos \theta_b) - \pi^2 V_d / 2) / \pi \omega L_s] \quad (5)$$

Since $I_d = V_d / R_L$, another relationship between and θ_b can be got and given by (6).

$$V_d = (V_s(2\sin \theta_b + \pi \cos \theta_b) / (\pi(\omega L_s / R_L + \pi/2))) \quad (6)$$

Supported the 2 relationships between V_d and θ_b , they'll be obtained from (4) and (6). The expression of θ_b is given by (7), then the expression of V_d also can be derived. Equation (7) indicates that the phase shift between u_s and u_{rec} (or i_{rec}) is especially set by L_s and R_L , and not reliable on WCS parameters. Since amplitudes of u_{rec} and i_{rec} are proportional to the u_s , we'll say that the parameters of WCS have less effect on the rectifier circuit, then the rectifier load are typically decoupled to analysis its equivalent input resistivity. The rectifier circuit consists of a resistance R_L (7). However, this equivalent relationship is simply appropriate for (7) and can't be used for the other half at intervals the rectifier load analysis.

$$\theta_b = \arctan(\omega L_s / R_L) \quad (7)$$

After obtaining V_d and θ_b , full response of the rectifier circuit at intervals the positive 0.5 cycle square measure usually calculated by (8); wherever, $\Phi(t)$ is that the characteristic matrix of rectifier circuit; the half before the sign is employed for locating zero-input response, and thus the other half is employed for locating zero-state response. On the thought of (8), time domain expressions of u_{rec} and i_{rec} square measure usually obtained, in line with the symmetry of their waveforms.

$$x(t) = \Phi(t)x(0) + \int_0^t \Phi(\tau)Bu(t - \tau)d\tau$$

$$= e^{At} \begin{bmatrix} 0 \\ V_d \end{bmatrix} + \int_0^t e^{A\tau} B \begin{bmatrix} V_s \sin(\omega(t - \tau) + \theta_b) \\ V_{dio} \end{bmatrix} d\tau \quad (8)$$

Finally, the basic wave amplitudes and part angles of u_{rec} and i_{rec} are calculated through Fourier transform, and outlined as U_{rec_fd} , I_{rec_fd} , φ_{urec_fd} , and φ_{irec_fd} . So, the equivalent input physical phenomenon of WCS rectifier load square measure getting to tend by (9); wherever, R_e and L_e square measure series equivalent resistance and inductance of the rectifier load, however the harmonic input impedances also can be obtained from FT. Moreover, the calculation method

suggests R_e and L_e square measure getting to be suffering from the parameters of the rectifier circuit

$$R_e = (U_{rec_fd} / I_{rec_fd}) \cos(\varphi_{rec_fd} - \varphi_{irec_fd}),$$

$$L_e = (U_{rec_fd} / I_{rec_fd}) \sin(\varphi_{rec_fd} - \varphi_{irec_fd}) / \omega \quad (9)$$

To sum up, the on top of study suggests that the rectifier load equivalent electric resistance contains each resistance and inductance elements. Also, the series equivalent resistance and inductance area unit typically severally calculated through parameters of rectifier circuit, then the results area unit primarily not suffering from different WCS parameters. So, the rectifier load area unit typically decoupled with different elements of WCS, and make system style easier.

3. COMPENSATION NETWORK DESIGN

Since the rectifier load has been decoupled with parts of WCS, a new compensation network style has been designed to carry out the rectifier load analysis and a few of existing researches [10-12]. Moreover, the projected technique can additional decouple the first and secondary aspect style, and build the WCS compensation network style simpler. As same as a result of the rectifier load analysis, the dual-side LCC compensation networks square measure used here. The rectifier input inductance L_s need to be giant enough to stay the rectifier operating in CCM state as mentioned on top of, therefore we'll confirm it before the compensation network style. Also, the first aspect compensation inductance L_p is assumed to be familiar, and solely the four compensation capacitors square measure utilized within the designing technique throughout this section.

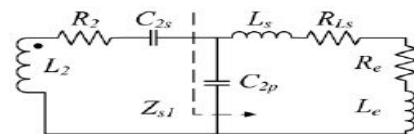


Fig. 4. Equivalent circuit of the system secondary aspect, considering rectifier load equivalent electric resistance

The secondary aspect is mentioned, and its equivalent circuit is shown in Fig.4; where, the series equivalent resistance R_e and equivalent inductance L_e are used to specify the rectifier load; R_2 is resistance of the receiving coil. As shown in Fig.4, Z_{s1} is the impedance of secondary side of the electrical resistance where C_{2s} is the series compensation device, and its expression is given by (10); wherever,

$$R_e' = R_e + R_{Ls}$$

$$L_e' = L_e + L_s$$

$$\text{re}(Z_{s1}) = \text{Fehler!},$$

$$\text{im}(Z_{s1}) = \text{Fehler!} \quad (10)$$

So, the efficiency can be calculated as in (11); where, η_c is efficiency of load from converter output to rectifier load impedance; R_1 is resistance of the sending coil;

$$X_{se} = \text{im}(Z_{s1}) + \omega L_2 - 1 / (\omega C_{2s}).$$

$$\eta_c = \text{Fehler!} \quad (11)$$

Equation (11) indicates that two conditions should be satisfied to get maximum output with high efficiency. One is $X_{se}=0$ to keep the divisor of η_c to a lowest possible value. The opposite is that the load resistance of the receive coil is same as resistance R_{opt} , as given by (12); wherever, R_{opt} area unit obtained from the derivation of η_c , when $X_{se}=0$.

$$re(Z_{s1}) = R_{opt} = \sqrt{R_2^2 + \omega^2 M^2 R_2 / R_1} \tag{12}$$

Using equations (10) & (12), the secondary aspect parallel compensation capacitance C_{2p} area unit can be given by (13), using C_{2p} and $X_{se}=0$, the secondary aspect series compensation capacitance C_{2s} also can be calculated. The secondary aspect compensation capacitors area unit usually designed dependent on primary side, and the maximum efficiency is achieved.

$$eq \setminus f (\omega L_e' + \sqrt{\omega^2 L_e'^2 - (R_e'^2 + \omega^2 L_e'^2) (1 - \frac{R_e'}{R_{opt}})}) / \omega (R_e'^2 + \omega^2 L_e'^2) \tag{13}$$

Then, the primary side is studied, and its equivalent circuit is shown in Fig.5; where, u_{inv} is converter output equivalent voltage source; R_{Lp} is stray resistances of L_p ; R_{es} is that the equivalent resistance of the secondary side, once C_{2s} and C_{2p} area unit neat, and $R_{es} = \omega^2 M^2 / (R_{opt} + R_2)$.

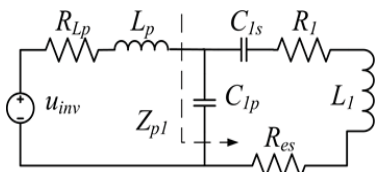


Fig.5, Z_{p1} is defined because the impedance after the first side compensation inductor L_p , and its

$$re(Z_{p1}) = \text{Fehler!},$$

$$im(Z_{p1}) = \text{Fehler!} \tag{14}$$

As shown in Fig.5, Z_{p1} is the impedance of primary side after inductor L_p , and as shown in (14); wherever,

$$X_{pe} = \omega L_1 - 1/(\omega C_{1s}) - 1/(\omega C_{1p});$$

The Primary side consists of two compensating capacitors. The two circuits can be created, one with WCS rated output power, as shown in equation (15); wherever, U_{inv} is that the RMS value of u_{inv} ; P_{or} is that the rated WCS output power; η_r is that the rated WCS efficiency.

$$U_{inv}^2 / re(Z_{p1}) = P_{or} / \eta_r \tag{15}$$

The second parameter is the specific inductance in soft switching mode of converter. The second parameter is as given by (16); wherever, L_{soft} is that the inductance required for converter soft shift.

$$im(Z_{p1}) / \omega + L_p = L_{soft} \tag{16}$$

Solving equations (15) & (16), the values of compensation capacitors C_{1s} and C_{1p} area are calculated, that's not affected by secondary design.

4. LOAD ESTIMATION METHODS

The rectifier load analysis results are usually used for system load estimation that adopting the high frequency signals in WCS. A quality load estimation ways are typically supported the pure resistance load, and conjointly want the high frequency voltage and current at an identical time [15-17]. The voltage and current sensors or probes can have completely different section delays at the high frequency vary, alongside those utilized in oscilloscopes and power analyzers. These completely different section delays can cause some deviations of the section between the measured voltage and current, and have an impact on the accuracy of the electrical resistance calculation, particularly once the section is on the brink of 90° , so on unravel this downside, we tend to propose a load estimation technique supported the secondary side high frequency voltages, the precise method is as follows: first, the positive zero crossings of the rectifier input voltage (u_{rec}) then the voltage before rectifier input device (the voltage on C_{2p} for LCC topology) are detected, therefore on get the positive zero crossing times. Then, outline the positive zero crossing time of the voltage before rectifier input device as t_{ucs} , then the next positive zero crossing time of the rectifier input voltage as t_{urs} . So, the load estimation expression is given by (17), in step with the association shown in (7). Finally, since WCS has been designed before load estimation, the worth of the rectifier input device L_s are usually measured, and system angle frequency ω is additionally best-known. So, the calculable load R_{L_Sesti} are usually calculated through (17).

$$R_{L_Sesti} = \omega L_s / \tan(\omega(t_{urs} - t_{ucs})) \tag{17}$$

The planned secondary side load estimation technique has thought of the influence of the WCS rectifier load. Also, solely high frequency voltages square measure utilized during this method; no current is adopted. Hence, it'll avoid the deviations introduced by completely different section delays between measured voltage and current. Besides, the planned technique solely detects the positive zero crossing times, however doesn't would really like the voltage amplitudes or RMS values. This might bring some simplifications to the corresponding measurements and calculations.

However, the measured signals still got to be transmitted to the first facet by wireless communication in most cases, used for system improvement or management, thus on avoid the issues brought by wireless communication, we've a bent to more recommend a load estimation technique supported the first facet high frequency voltages. Here, the converter output voltage (u_{inv}) then the voltage once converter output device (the voltage on C_{1p} for LCC topology) measure adopted, outline the important voltage transfer function between the converter output voltage then the voltage of converter output device, then the essential voltage transfer perform between the voltage before rectifier input device and also the rectifier input voltage as G_s . So, we'd wish to seek out a relationship between G_s and G_p , then the measured primary voltages calculates θ_b . To calculate this, some WCS acts as two port network[11]. Hence, the coupling coils and compensation capacitors comprise of a two-port network as shown in Fig.6.

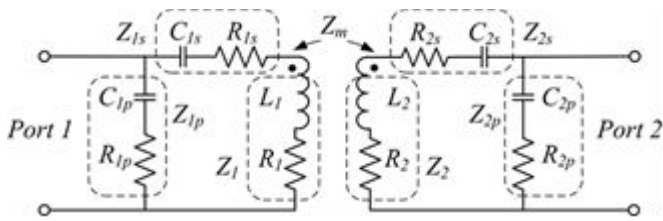


Fig. 6. Schematic of the equivalent two-port network and its parameters.

According to Fig.6, the parameters of the equivalent two-port network area unit typically calculated and given by (18a).

$$Z_{11} = Z_{1p} ((Z_1 + Z_{1s})(Z_2 + Z_{2s} + Z_{2p}) - Z_m^2) / \text{den},$$

$$Z_{12} = Z_{21} = Z_{1p} Z_{2p} Z_m / \text{den}, \tag{18a}$$

$$Z_{22} = Z_{2p} ((Z_2 + Z_{2s})(Z_1 + Z_{1s} + Z_{1p}) - Z_m^2) / \text{den}$$

Where, $Z_m = j\omega M$, and the denominator den is defined by (18b)

$$\text{den} = (Z_1 + Z_{1s} + Z_{1p})(Z_2 + Z_{2s} + Z_{2p}) - Z_m^2 \tag{18b}$$

Then, the affiliation between G_s and physician area unit typically got and given by (19a), supported the electrical resistance parameters of the equivalent two-port network.

$$G_s = (n_1 G_p + n_2) / (d_1 G_p + d_2) \tag{19a}$$

$I_{L2(s)}$ is that the reference current of L_2 V_{DC} is that the motor voltage, agency is that the device DC motor, D is that the duty cycle, at intervals the frequency vary, the affiliation Where, the coefficients n_1 , n_2 , d_1 , and d_2 area unit outlined by (19b); wherever, $Z_p = RL_p + j\omega L_p$; $Z_s = RL_s + j\omega L_s$.

$$n_1 = Z_{12} Z_{21} - Z_{11} Z_{22}, \quad d_2 = (Z_{11} + Z_p)(Z_{22} + Z_s) - Z_{12} Z_{21},$$

$$n_2 = Z_p Z_{22} + Z_{11} Z_{22} - Z_{12} Z_{21}, \quad d_1 = Z_{12} Z_{21} - Z_{11} (Z_{22} + Z_s) \tag{19b}$$

Furthermore, the amplitudes and section angles of the chosen voltages calculated on the primary side, then the transfer perform G_p value typically obtained. Outline the amplitude of G_p as Php , then the phase shift of G_p as Php . So, θ_n , which is the phase shift of G_s , also as θ_d , that's that the phase angle denominator of G_s . Their expressions square measure given by (20)

$$\theta_n = \arctan \frac{\text{Amp.amn1.sin(Php+phn1)+imn2}}{\text{Amp.amn1.cos(Php+phn1)+ren2}},$$

$$\theta_d = \arctan \frac{\text{Amp.amd1.sin(Php+phd1)+imd2}}{\text{Amp.amd1.cos(Php+phd1)+red2}} \tag{20}$$

Where, a_{mn1} and p_{hn1} calculates the magnitude and phase shift of n_1 ; a_{md1} and p_{hd1} calculates the magnitude and phase shift of d_1 ; ren_2 and imn_2 are in the complex form for n_2 ; red_2 and imd_2 are in complex form for d_2 ; they'll be calculated through (18) and (19), consistent with the measured values of the WCS parameters.

Finally, we'll get the section of G_s , then the calculable load R_{L_Pesti} can be derived using (21). Moreover, the derivation method suggests that R_{L_Pesti} affects WCS parameters, like mutual-inductance M , compensation capacitances C_{1s} , C_{1p} , C_{2s} , C_{2p} , and so on. Hence, the validation of parameters is done, however similar with the

case of the rectifier equivalent load calculation methodology, the theoretical ways cannot provide a simple and clear due to analyze the validation.

$$R_{L_Pesti} = \omega L_s / \tan(\theta_n - \theta_d) \tag{21}$$

Developed from the upper than secondary load estimation methodology, the projected primary load estimation methodology has additionally thought of the influence of the rectifier load. Meanwhile, it solely adopts high frequency voltages, and will avoid the part delay deviations, too. The excellence is that this system should live voltage amplitudes. However, on the contrary, it doesn't need wireless communication between the first and secondary sides. So, it's some benefits in heat unit applications.

5. SIMULINK MODEL & RESULTS

A. Simulink model

A WCS or EV wireless charging model is developed to verify the rectifier load analysis results then the projected strategies. Its configuration is shown inside the photograph in Fig.7 a 3 phase supply is appointed as supply. System load could even be a full-bridge diode rectifier with wireless charging coil.

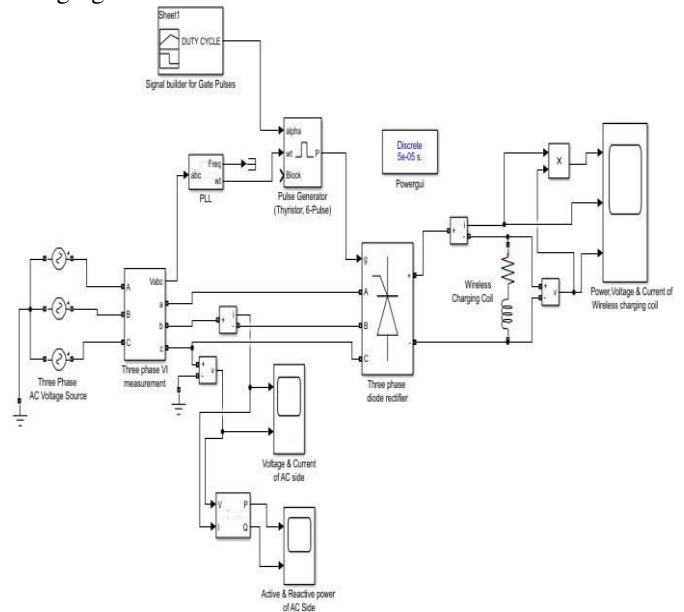


Fig. 7. Simulink Model for load analysis for rectifier

The model is meant with rated input AC voltage four hundred V. The load is 3 phase diode bridge rectifier with wireless charging coil. The input current, Voltage & power are measured at supply side whereas output current, voltage & dc power is measured at load side. Above model build the system deliver the good performances, like rated output power, high efficiency, converter soft change, etc.

B. Results

Figure 8, 9 & 10 shows the waveforms for Voltage, Current, Power, input voltage & current, voltage & Power of the load.

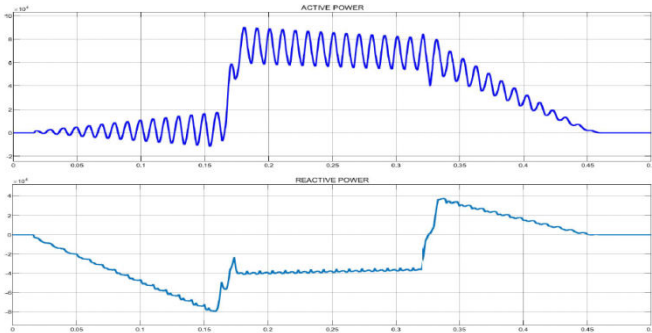


Fig 8. Active power & reactive power

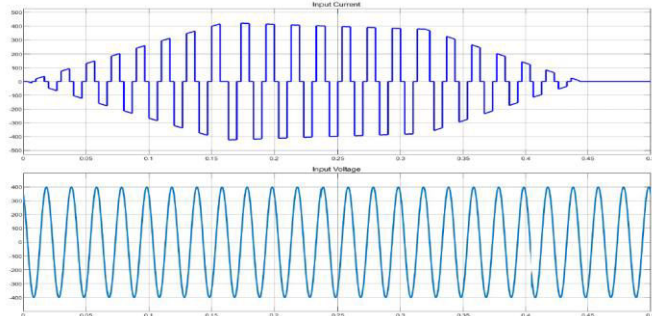


Fig 9. Input Voltage & Input Current

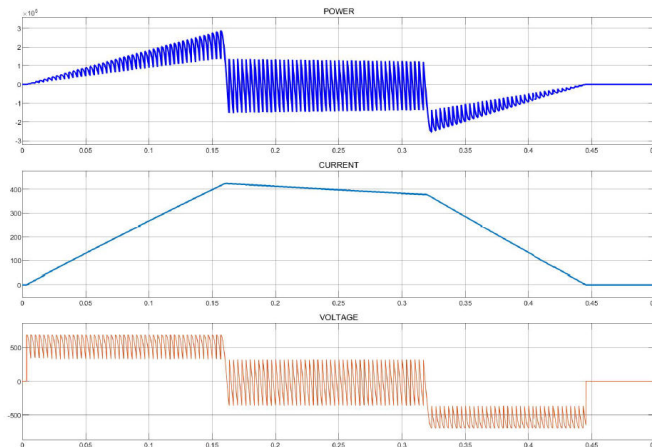


Fig 10. Power, Current & voltage at rectifier output

CONCLUSIONS

This paper presents a scientific analysis of the rectifier load used for heat unit wireless charging system. The rectifier load model has been established to calculate the output power of wireless charging coil, supported the rectifier load analysis, a compensation network style methodology is projected to know the specified. The simulation results have shown the subsequent conclusions: the rectifier load is extremely filled with system load resistance then the projected load estimation ways have sensible accuracy, however still need to be improved in additional research; the projected rectifier load calculation methodology and system load estimation ways all have sensible lustiness, on conditions of WCS parameter variations. though the works throughout this paper are conducted supported the precise system, they go to be extended to additional applications, like wireless charging systems with different rectifier or compensation network topologies, etc. they're getting to be useful for system style and management to make heat unit wireless charging systems reach stable operation and high performance.

REFERENCES

- [1] Y. Guo, and L. Wang, "Rectifier load analysis for electric vehicle wireless charging system," *IEEE Transactions on Industrial Electronics* 65.9 (2018): 6970-6982.
- [2] W. X. Zhong, and S. Y. R. Hui, "Maximum energy efficiency tracking for wireless power transfer systems," *IEEE Trans. Power Electron.*, vol. 30, no. 7, pp. 4025-4034, Jul. 2015.
- [3] S. Q. Li, and C. C. Mi, "Wireless power transfer for electric vehicle applications," *IEEE J. Emerg. Sel. Topics Power Electron.*, vol. 3, no. 1, pp. 4-17, Mar. 2015.
- [4] D. Thenathayalan, and J. H. Park, "Wide-air-gap transformer model for the design-oriented analysis of contactless power converters," *IEEE Trans. Ind. Electron.*, vol. 62, no. 10, pp. 6345-6359, Oct. 2015.
- [5] M. Fu, Z. Tang, M. Liu, C. Ma, and X. Zhu, "Full-bridge rectifier input reactance compensation in megahertz wireless power transfer systems," in *Proc. 2015 WoW*, 2015, pp. 1-5.
- [6] Y. Akihara, T. Hirose, S. Masuda, N. Kuroki, M. Numa, and M. Hashimoto, "Analytical study of rectifier circuit for wireless power transfer systems," in *Proc. ISAP*, 2016, pp. 338-339.
- [7] H. C. Li, K. P. Wang, L. Huang, W. J. Chen, and X. Yang, "Dynamic modeling based on coupled modes for wireless power transfer systems," *IEEE Trans. Power Electron.*, vol. 30, no. 11, pp. 6245-6253, Nov. 2015.
- [8] H. T. Shi, J. D. Mao, X. S. Li, and J. T. Pan, "Modeling and analysis of impedance for uncontrolled rectifier based nonlinear load," in *Proc. CCDC*, 2016, pp. 1770-1775.
- [9] Q. Lei, M. Shen, V. Blasko, and F. Z. Peng, "A generalized input impedance model of three phase diode rectifier," in *Proc. APEC*, 2013, pp. 2655-2661.
- [10] S. Q. Li, W. H. Li, J. J. Deng, T. D. Nguyen, and C. C. Mi, "A double-sided LCC compensation network and its tuning method for wireless power transfer," *IEEE Trans. Veh. Technol.*, vol. 64, no. 6, pp. 2261-2273, Jun. 2015.
- [11] Q. W. Zhu, L. F. Wang, and C. L. Liao, "Compensate capacitor optimization for kilowatt-level magnetically resonant wireless charging system," *IEEE Trans. Ind. Electron.*, vol. 61, no. 12, pp. 6758-6768, Dec. 2014.
- [12] J. W. Kim, D. H. Kim, and Y. J. Park, "Analysis of capacitive impedance matching networks for simultaneous wireless power transfer to multiple devices," *IEEE Trans. Ind. Electron.*, vol. 62, no. 5, pp. 2807-2813, May 2015.
- [13] J. Kim, and J. Jeong, "Range-adaptive wireless power transfer using multiloop and tunable matching techniques," *IEEE Trans. Ind. Electron.*, vol. 62, no. 10, pp. 6233-6241, Oct. 2015.
- [14] W. H. Li, H. Zhao, S. Q. Li, J. J. Deng, T. Z. Kan, and C. C. Mi, "Integrated LCC compensation topology for wireless charger in electric and plug-in electric vehicles," *IEEE Trans. Ind. Electron.*, vol. 62, no. 7, pp. 4215-4225, Jul. 2015.
- [15] J. P. W. Chow, H. S. H. Chung, and C. S. Cheng, "Use of transmitter-side electrical information to estimate mutual inductance and regulate receiver-side power in wireless inductive link," *IEEE Trans. Power Electron.*, vol. 31, no. 9, pp. 6079-6091, Sep. 2016.
- [16] M. Feliziani, T. Campi, S. Cruciani, F. Maradei, U. Grasselli, M. Macellari, and L. Schirone, "Robust LCC compensation in wireless power transfer with variable coupling factor due to coil misalignment," in *Proc. 2015 IEEEIC*, 2015, pp. 1181-1186.
- [17] M. Liu, Y. Qiao, and C. B. Ma, "Robust optimization for a 6.78-MHz wireless power transfer system with class E rectifier," in *Proc. 2016 WoW*, 2016, pp. 88-94.